Casimir-Polder force on a two-level atom in a structure containing metamaterials

Jingping Xu,[1,2] M. Alamri,[2,3] Yaping Yang,[1] Shi-Yao Zhu,[3] and M. Suhail Zubairy[3,4]

[1]*MOE Key Laboratory of Advanced Micro-Structured Materials, School of Physics Science and Engineering, Tongji University, Shanghai 200092, China*

[2]*The National Centre for Applied Physics, KACST, Riyadh 11442, Saudi Arabia*

[3]*Beijing Computational Science Research Center, Beijing 100084, China*

[4]*Institute for Quantum Science and Engineering and Department of Physics and Astronomy, Texas A&M University, College Station, Texas 77843, USA*

(Received 20 January 2014; published 27 May 2014)

We study the Casimir-Polder (CP) force on an excited cold two-level atom in structures containing metamaterials. We adopt two kinds of metamaterials: left-handed materials (LHMs) and zero-index materials (ZIMs). The CP force on an excited atom can be divided into two parts: the dispersive force that responds to all frequencies of the electromagnetic mode and the resonant force, which is determined by the frequency at the atomic transition. Left-handed materials and ZIMs can significantly modify the resonant part of the CP force due to their unique character. It is found here that the presence of LHMs can enhance the force on the atom far away from the surface due to its phase compensation, while the presence of ZIMs can lead to a force that is independent of dipole orientation. The Casimir effect within the combination of LHMs and ZIMs leads us to realize a potential well that is insensitive to the orientation of atomic dipole. Due to the spontaneous decay, the resonant part of the CP force disappears eventually; however, the decay at the position with maximum force is inhibited. Therefore, during the time evolution, there are special positions (focuses) at which the force is significant for a longer time. Our results show the trap effect that can work on an atom with arbitrary dipole orientation. This provides a method to either trap or reflect an atom in a position far away from surface.

DOI: 10.1103/PhysRevA.89.053831 PACS number(s): 42.50.Nn, 12.20.−m, 42.50.Wk, 34.35.+a

I. INTRODUCTION

The Casimir-Polder (CP) force refers to the force between neutral atoms and materials [1]. It originates from the quantum fluctuation of both the field and dipole momentum. The CP force has several applications in atomic optics and has been extensively investigated for the case when the atom is in the ground state [1–7]. To mention a few applications, it can be used to make the transmission gratings for atomic matter waves and to realize atomic Mach-Zehnder-type interferometers [2]. The combination of the Casimir force and gravitational force can be used to realize the flat quantum reflective mirror, which provides a focusing mechanism [3]. It also should be taken into account to construct evanescent-wave elements for atom guiding [4]. Meanwhile, the Casimir force can be a disturbing factor of nanodevices, which leads to an undesired sticking of small objects to the surface [5] and diminishes the depth of magneto-optical traps when near the surface [6]. The influence of the nanostructure on the Casimir-Polder potential, i.e., an atom near a monolayer made by the periodically arranged metallic and dielectric nanospheres, has also been analyzed [7]. All the aforementioned applications are based on the force that is acting on an atom in the ground state. However, the excited-state calculations have also attracted plenty of interest [8–13]. It has been shown that the Casimir-Polder force on an excited atom is much stronger than that on the ground state and varies sinusoidally with distance from the surface [14]. As a major achievement, the method has shown that the force on excited atoms can be repulsive [15].

The force on the atom in the ground state is dispersive and frequency dependent over a wide range. However, the force on the excited state is mainly related to the frequency region near the atomic transition frequency. Therefore, it is convenience to control the force on an excited atom by tailoring the electromagnetic property of material near atom. In the usual material, the force on the excited atom decreases as $1/r$ (r is the distance of the atom from the surface) with oscillations [13,14].

In this paper we propose a structure that helps enhance the Casimir-Polder force on an excited atom even when it is several wavelengths away from the surface. The structure is made of metamaterials that are obtained by combining the left-handed metamaterials (LHMs) and high-reflectivity materials. We will compare two kinds of highly reflective materials: metal and zero-index metamaterials (ZIMs). It is found that the force on the atom near LHMs mounted on a metal is dependent on the atomic dipole orientation, while the force near LHMs mounted on ZIMs is nearly independent of the dipole's orientation. The LHMs and ZIMs are both different kinds of manmade materials [16–25]. Left-handed metamaterials possess negative permittivity, negative permeability, and negative refractive index simultaneously, while the indices of ZIMs are zero at the frequency of interest. The name left-handed metamaterial comes from the observation that the electric field, the magnetic field, and the wave vector form a left-handed triplet within it [16]. Some unusual phenomena such as reverse Doppler shift, reverse Cerenkov radiation, and reverse light pressure are predicted in LHMs [16]. An important potential application of the LHMs is the perfect lens that can focus both the propagation waves and the evanescent waves [17]. It was found that the spontaneous emission of an atom can be inhibited completely under certain conditions when the atom is placed in front of an ideal LHM layer ($\varepsilon = -1$, $\mu = -1$) and mounted on a perfect mirror [18]. Zero-index metamaterials in which $\varepsilon = \mu = 0$, $\varepsilon = 0$, or $\mu = 0$ have attracted interest due to their unique electromagnetic properties such as tailoring the radiation phase patterns [19], squeezed electromagnetic waves [20], directional emission [21], cloaking [22], and Dirac

 ©2014 American Physical Society

conelike dispersions [23,24]. Furthermore, Yannopapas and Vanakaras found the Dirac point in the dispersion relation of a three-dimensional crystal made by gold nanoparticles embedded in high-index dielectric materials and pointed out that such Dirac-type dispersion lines of photon modes is the result of the gapless transition from a negative to a positive index band [25]. Recently, several important features of the $n = 0$ structures for visible light were confirmed by using a metal-insulator-metal waveguide at the cutoff [26]. The influence of LHMs on the Casimir-Polder potential of excited atoms [27] has been investigated and it was found that under appropriate conditions, the superlens-type geometry could form a barrier near the surface. Evidently, metamaterials (including LHMs, ZIMs, and nanostructures) have many promising applications when it comes to the use of quantum optical phenomena such as enhanced quantum interference [28–30], Casimir force [31], a single-photon source [32], and prolonged entanglement [33,34]. One of the main goals of this paper is to use the focusing effect of LHMs to control the Casimir-Polder force on an excited-state atom.

This paper is organized as follows. In Sec. II we introduce the model and theorem needed to explore the Casimir-Polder force. In Sec. III we adopt several parameters that are needed to calculate the Casimir- Polder force on an initially excited atom and show the dynamical evolution. In Sec. IV we present a summary.

II. MODEL AND FORMULAS

We consider two structures to study the influence of LHMs on the Casimir-Polder force that is acting on an atom near the surface of that structure. The first structure is shown in Fig. 1(a), in which a LHM slab with ε_A, μ_A, and thickness d_A is mounted on high-reflectivity material with ε_M and μ_M. The second structure is shown in Fig. 1(b), in which two structures of Fig. 1(a) form a cavity with thickness d_0.

A two-level atom with transition frequency ω_{10} and dipole momentum $\mathbf{d}_{10}$ is placed at position $\mathbf{r}_a = (0,0,z_a)$. The range of z_a is limited by $z_a > 0$ in Fig. 1(a) and $z_a \in [0,d_0]$ in Fig. 1(b). The atom is assumed stationary, so there is no need to consider the movement of the atom.

The initial state of the system is that the atom is prepared in an excited state and the electromagnetic field is in a vacuum state. Starting from such an initial state, the Casimir-Polder force is genuinely time dependent. Therefore, the best method to calculate the time-dependent force is to adopt the Heisenberg method, which gives the operator of the electromagnetic force acting on an atom, which then enables us to calculate its expectation values.

Here we adopt the method presented in Ref. [13] to get the evolution of the expectation value of electromagnetic force operator acting on a stationary atomic electric dipole in the long-wavelength approximation, which is given by [13]

$$\mathbf{F} = \langle \hat{\mathbf{F}}_L \rangle = \left\langle \left\{ \nabla[\hat{\mathbf{d}} \cdot \hat{\mathbf{E}}(\mathbf{r})] + \frac{d}{dt}[\hat{\mathbf{d}} \times \hat{\mathbf{B}}(\mathbf{r})] \right\}_{\mathbf{r}=\mathbf{r}_a} \right\rangle. \quad (1)$$

The first term refers to the dipole force by the electric field, while the second term refers to the Lorentz force. The contribution of the magnetic dipole of an atom has been discarded due to its ignorable effect compared to the contribution of the electric dipole.

Equation (1) provides a basis for the calculation of the electromagnetic force acting on nonmagnetic atoms regardless of the state of the atom and the body-assisted field. For the initially excited two-level atom, under the Green's tensor quantization [35], after expressing the electromagnetic-field operators by the operator of the atomic dipole through the Heisenberg equation, we get the force evolution under the Markov approximation as [13]

$$\begin{aligned} \mathbf{F}(t) &= \sigma_{11}(t)\mathbf{F}_1(\mathbf{r}_a) + \sigma_{00}(t)\mathbf{F}_0(\mathbf{r}_a) \\ &\approx e^{-\Gamma(z_a)t}\mathbf{F}_1(z_a) + (1 - e^{-\Gamma(z_a)t})\mathbf{F}_0(z_a), \end{aligned} \quad (2)$$

where $\sigma_{11}(t)$ is the probability of the atom in the excited state that decays exponentially with decay rate $\Gamma(z_a)$ and $\sigma_{00}(t) = 1 - e^{-\Gamma t}$ is the probability of the atom being in the ground state; they satisfy the condition $\sigma_{00}(t) + \sigma_{11}(t) = 1$. The time-independent vectors $\mathbf{F}_1(z_a)$ and $\mathbf{F}_0(z_a)$ represent the forces acting on the excited and the ground state of the atom, respectively. The force $\mathbf{F}_1(z_a)$ consists of two parts: a resonant part $F_1^r(z_a)$ and an off-resonant part $F_1^{or}(z_a)$ given by

$$\mathbf{F}_1(z_a) = \hat{e}_z\left[F_1^{or}(z_a) + F_1^r(z_a)\right], \quad (3)$$

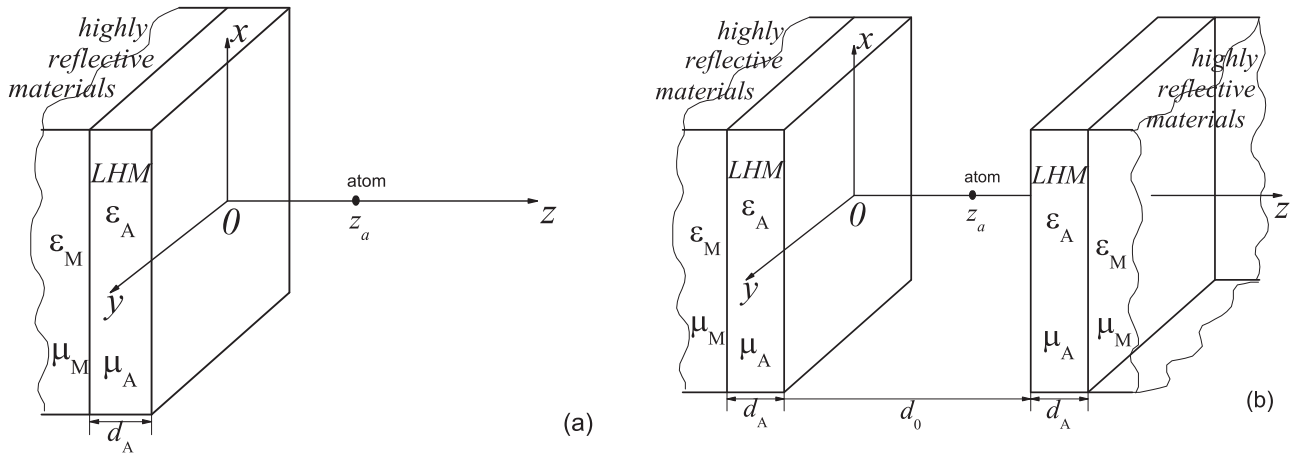

FIG. 1. (a) Single LHM-mirror structure and (b) a cavity made by LHMs.

$$F_1^r(z_a) = 2\mu_0\omega_{10}^2\mathbf{d}_{10}\cdot\frac{\partial}{\partial z}\left[\mathrm{Re}\overleftrightarrow{\mathbf{G}}^{(1)}(z,z_a,\omega_{10})\right]\cdot\mathbf{d}_{10}|_{z=z_a}, \quad (4)$$

$$F_1^{or}(z_a) = \frac{2\mu_0}{\pi}\int_0^\infty \frac{d\xi\omega_{10}\xi^2}{\omega_{10}^2+\xi^2}\mathbf{d}_{10}\cdot\frac{\partial}{\partial z}\cdot\left[\overleftrightarrow{\mathbf{G}}^{(1)}(z,z_a,i\xi)\right]\cdot\mathbf{d}_{10}|_{z=z_a}. \quad (5)$$

The force acted on the atom in the ground state $\mathbf{F}_0(z_a)$ consists of only off-resonant part, which is

$$\mathbf{F}_0(z_a) = -\hat{e}_z F_1^{or}(z_a). \quad (6)$$

The off-resonant part of the force $F_1^{or}(z_a)$ is the dispersive part of the force. According to Eq. (6), the dispersive part acting on the excited atom has the same amplitude as that acting on the ground-state atom, but with opposite sign. Therefore, an attractive force takes place on the atom in the ground state near a dielectric surface, while a repulsive force happens for an excited atom near the same surface [15]. The decay rate determines the evolution of the force, which is

$$\Gamma(\mathbf{r}_a) = \Gamma(z_a) = \frac{2\mu_0}{\hbar}\omega_{10}^2\mathbf{d}_{01}\cdot\mathrm{Im}\overleftrightarrow{\mathbf{G}}(z_a,z_a,\omega_{10})\cdot\mathbf{d}_{10}. \quad (7)$$

All the aforementioned quantities relate to the electromagnetic Green's tensor. This tensor, related to the environments shown in Fig. 1, is given by

$$\overleftrightarrow{\mathbf{G}}(z,z_a,\omega) = \frac{i}{2(2\pi)^2}\int d^2\mathbf{q}\frac{1}{K_z}\sum_{\sigma=s,p}\left[\left(\mathbf{e}_\sigma^+ e^{iK_z(z-z_a)}\Theta(z-z_a) + \frac{\mathbf{e}_\sigma^+ r_L^\sigma r_R^\sigma e^{iK_z(z+2d_0-z_a)} + \mathbf{e}_\sigma^- r_R^\sigma e^{iK_z(2z_R-z_a-z)}}{1-r_L^\sigma r_R^\sigma e^{i2K_z d_0}}\right)\mathbf{e}_\sigma^+ + \left(\mathbf{e}_\sigma^- e^{-iK_z(z-z_a)}\Theta(z_a-z) + \frac{\mathbf{e}_\sigma^+ r_L^\sigma e^{iK_z(z+z_a-2z_L)} + \mathbf{e}_\sigma^- r_R^\sigma r_L^\sigma e^{iK_z(2d_0+z_a-z)}}{1-r_L^\sigma r_R^\sigma e^{i2K_z d_0}}\right)\mathbf{e}_\sigma^-\right], \quad (8)$$

where $\boldsymbol{q}$ is the wave-vector component in the vacuum that is parallel to the surface and K_z is the component along the z axis. They both satisfy $q^2+K_z^2=\omega^2/c^2$. Here r_L^σ (r_R^σ) is the reflection coefficient of the left (right) structure for σ polarization, which can be expressed by the multiple-beam reflection, $\mathbf{e}_\sigma^{+(-)}$ is the unit vector of the σ polarization field propagating along the positive (negative) z axis in the vacuum, $\mathbf{e}_s^\pm = \mathbf{e}_q\times\mathbf{e}_z = \sin\phi\mathbf{e}_x - \cos\phi\mathbf{e}_y$, and $\mathbf{e}_p^\pm = (\pm K_z\cos\phi\mathbf{e}_x \pm K_z\cos\phi\mathbf{e}_y + q\mathbf{e}_z)/K$. The scattering part of the Green's tensor related to the force can be expressed as

$$\overleftrightarrow{\mathbf{G}}^{(1)}(z,z_a,\omega) = \frac{i}{2(2\pi)^2}\int d^2\mathbf{q}\frac{1}{K_z}\times\sum_{\sigma=s,p}\left[\frac{r_R^\sigma e^{iK_z(2z_R-z_a-z)}}{1-r_L^\sigma r_R^\sigma e^{i2K_z d_0}}\mathbf{e}_\sigma^-\mathbf{e}_\sigma^+ + \frac{r_L^\sigma e^{iK_z(z+z_a-2z_L)}}{1-r_L^\sigma r_R^\sigma e^{i2K_z d_0}}\mathbf{e}_\sigma^+\mathbf{e}_\sigma^-\right]. \quad (9)$$

If the atomic dipole moment is parallel to the surface, i.e., $\mathbf{d}_{10}=d_{10}\mathbf{e}_x$, then

$$F_1^r(z_a) = B\mathrm{Re}\int_0^\infty dq\frac{q}{K^2}\left[\frac{r_R^s e^{iK_z(d_0-2z_a)} - r_L^s e^{iK_z 2z_a}}{1-r_L^s r_R^s e^{i2K_z d_0}} - \frac{K_z^2}{K^2}\frac{r_R^p e^{iK_z(2z_R-2z_a)} - r_L^p e^{iK_z(2z_a-2z_L)}}{1-r_L^p r_R^p e^{i2K_z d_0}}\right], \quad (10)$$

$$F_1^{or}(z_a) = -B\frac{1}{\pi}\int_0^\infty\frac{d\xi\xi^2}{\omega_{10}^2}\frac{\omega_{10}}{\omega_{10}^2+\xi^2}\int_0^\infty\frac{dqq}{K^2}\times\left[\frac{r_L^s e^{-b2z_a} - r_R^s e^{-b(d_0-2z_a)}}{1-r_L^s r_R^s e^{i2K_z d_0}} - \frac{b^2}{k^2}\frac{r_L^p e^{-b2z_a} - r_R^p e^{-b(d_0-2z_a)}}{1-r_L^p r_R^p e^{i2K_z d_0}}\right]. \quad (11)$$

However, when it is normal to the surface, i.e., $\mathbf{d}_{10}=d_{10}\mathbf{e}_z$, then

$$F_1^r(z_a) = B2\mathrm{Re}\int_0^\infty dq\frac{q^3}{K^4}\frac{r_R^p e^{iK_z(2z_R-2z_a)} - r_L^p e^{iK_z(2z_a-2z_L)}}{1-r_L^p r_R^p e^{i2K_z d_0}}, \quad (12)$$

$$F_1^{or}(z_a) = B\frac{2}{\pi}\int_0^\infty\frac{d\xi\xi^2}{\omega_{10}^2}\frac{\omega_{10}}{\omega_{10}^2+\xi^2}\times\int_0^\infty\frac{dqq}{K^2}\frac{q^2}{k^2}\frac{r_L^p e^{-b2z_a} - r_R^p e^{-b(d_0-2z_a)}}{D_p}, \quad (13)$$

where $B=\mu_0|d_{10}|^2\omega_{10}^4/4\pi^2c^2, K=\omega_{10}/c$, $k=\xi/c$, and $q^2-b^2=-k^2$. The atomic decay rate can be calculated in a similar manner. In this paper we mainly adopt Eqs. (10)–(13) and insert them into Eqs. (2), (3), and (6) to calculate the evolution of the Casimir-Polder force acting on the atom with different dipole orientations.

III. CALCULATION AND ANALYSIS

Before discussing the influence of LHMs on the Casimir-Polder force, we first check the result when the force is acting on an atom placed near a semispace dielectric. The susceptibility of the dielectric satisfies the Kramers-Kronig relation and can be described by the Drude-Lorentz model. Here we adopt

$$\varepsilon_A = \varepsilon_M = 1 + \frac{(0.8\omega_{10})^2}{(1.1\omega_{10})^2-\omega^2-i(0.001\omega_{10})\omega}, \quad \mu_A=\mu_M=1. \quad (14)$$

Therefore, the refractive indices at the atomic transition frequency are $\varepsilon_A(\omega_{10})=\varepsilon_M(\omega_{10})=4.05+i0.001$. The time-independent quantities $F_1(z_a)$ and $\Gamma(z_a)$, as functions of position z_a, are shown in Fig. 2. In the following we scale the

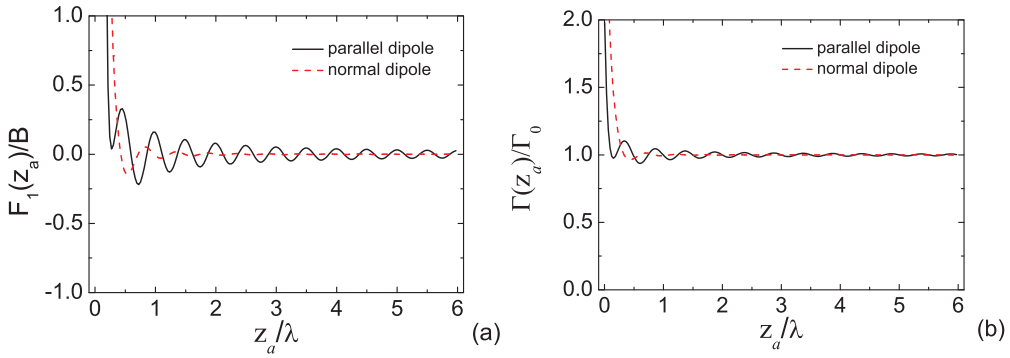

FIG. 2. (Color online) Initial excited atom near the dielectric semispace with the parameters from Eq. (14). (a) Time-independent force amplitude $\mathbf{F}_1(z_a)$ as a function of position. (b) Decay rate $\Gamma(z_a)$ as a function of position.

position unit using the atomic transition wavelength, i.e., $\lambda = 2\pi c/\omega_{10}$, while the unit of the decay rate is scaled to the decay rate when the atom is in free space, i.e., $\Gamma_0 = d_{10}^2\omega_{10}^3/3\pi\varepsilon_0\hbar c^3$.

From Fig. 2 it is clear that the force amplitude of the initial excited atom decreases sharply as the atom moves away from the surface in an oscillating behavior, for both normal and parallel dipoles. When $z_a > 0.5\lambda$, the force is small and inversely proportional to z_a^2, while the atomic decay rate tends to Γ_0. We find that the force on the normal dipole is weaker than that on the parallel dipole in general. Using Eq. (2), we can reconstruct the evolution of the Casimir-Polder force in which the resonant part of the force decreases exponentially with rate Γ_0 and the nonresonant part changes sign and finally we can see that the force is just the Casimir-Polder force acting on the ground-state atom. Such evolution indicates a rapid change when the atom is close to the surface due to a high decay rate. Hence, the force is significant only when the atom is near the surface.

A. Left-handed materials mounted on metal

Next we calculate the results for a single LHM-metal structure [see Fig. 1(a)]. The permittivity and permeability of the LHM slab are, respectively,

$$\begin{aligned}\varepsilon_A &= 1 + \frac{(0.8\omega_{10})^2}{(0.8246\omega_{10})^2 - \omega^2 - i(0.001\omega_{10})\omega},\\ \mu_A &= 1 + \frac{(0.8\omega_{10})^2}{(0.8246\omega_{10})^2 - \omega^2 - i(0.001\omega_{10})\omega}.\end{aligned} \tag{15}$$

Here the LHM has two characteristics that are distinct from the dielectric: one is the strong magnetic response, i.e., $\mu_A \neq 1$, and the other is the negative refractive index near the atomic transition frequency, i.e., $\varepsilon_A(\omega_{10}) = \mu_A(\omega_{10}) \approx -1.001 + i0.006$. The indices of the metal are chosen as

$$\varepsilon_M = 1 - \frac{(4\omega_{10})^2}{\omega^2}, \quad \mu_M = 1, \tag{16}$$

i.e., the susceptibility of the metal is negative and its refractive index is purely imaginary.

It should be pointed out that we adopt the effective-medium theory to describe the response of metamaterials near resonance with the Drude-Lorentz model [i.e., Eqs. (15) and (17)]. It is known that the real metamaterial consists of subwavelength microresonant elements [16–24]. After comprising the accurate numerical method with the effective-medium theory, it was found that the Drude-Lorentz model cannot exactly describe the response of metamaterials to the electromagnetic field in quantity due to the resonance-antiresonance coupling phenomena, the misshapen index profile near resonance, and the discrepancy between the effective refractive index and effective impedance at resonance [36]. Furthermore, the periodicity of the structure can also weaken the validity of the effective-medium theory when the wavelength of the electromagnetic wave is smaller than 30 space periods of the metamaterials [37]. However, the effective-medium theory agrees qualitatively with theoretical predictions and experimental results.

For the Casimir-Polder force, the resonant part (4) is much more significant that the dispersive part (5) when the atom is away from the surface [12]. Since the dispersion of the material affects only the dispersive part of the force, the choice of parameters of the Drude-Lorentz model has a tiny influence on the force acting on the excited atom. Therefore, the influence of the Drude-Lorentz model on the dispersive part of the force is therefore neglected in this paper. Next we insert these parameters into the Green's tensors of Eqs. (8) and (9) and calculate the time-independent quantities $F_1(z_a)$ and $\Gamma(z_a)$ as functions of position for $d_A = \lambda$ and $d_A = 2\lambda$. The results are presented in Figs. 3 and 4.

As the thickness of the LHM slab is $d_A = \lambda$, the focus point of the electromagnetic field at frequency ω_{10} is at $z_a = \lambda$. Therefore, the resonant part of the CP force can be modified significantly. In Fig. 3(a) it is clear that the amplitude of the time-independent force $F_1(z_a)$ has a different and significant behavior: It decays exponentially with distance near the surface and then starts to have a peak near $z_a = \lambda$. Simultaneously, the decay rate also tends to have the same important signature near the focus point where $z_a = \lambda$.

We can see this important behavior more clearly when we increase the thickness of the LHM slab to $d_A = 2\lambda$, as shown in Fig. 4. The amplitude of $F_1(z_a)$ no longer decreases monotonically with z_a and it has a revival behavior near the focus point $z_a = 2\lambda$. It can be seen, on comparing Figs. 4 and 3, that the profiles of both $F_1(z_a)$ and $\Gamma(z_a)$ near $z_a = d_A$ are nearly the same in these two cases except that in Fig. 3 the left part when $z_a < d_A$ is distorted by the surface. The common character of Figs. 3 and 4 is that the forces on the

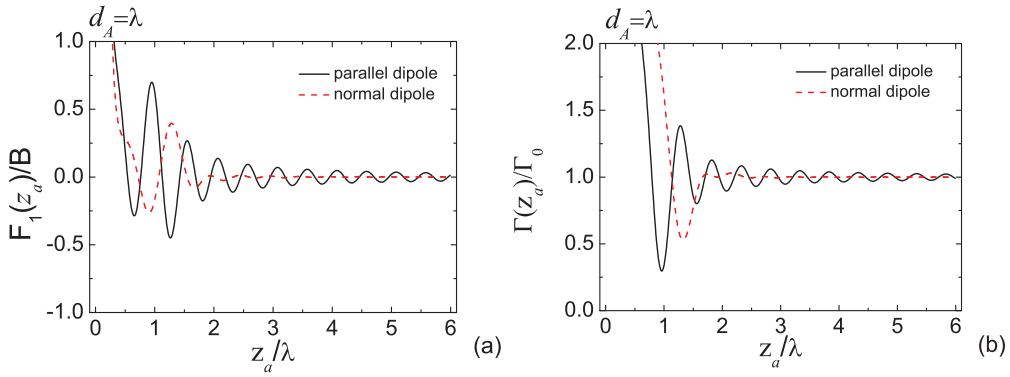

FIG. 3. (Color online) (a) Time-independent force amplitude $\mathbf{F}_1(z_a)$ and (b) atomic decay rate $\Gamma(z_a)$ as functions of position. Here an initially excited atom is placed near a LHM slab [as described by Eq. (26)] of thickness $d_A = \lambda$ that is mounted on metal [as described by Eq. (16)] as shown in Fig. 1(a).

atom are enhanced compared to the dielectric case in Fig. 2. When $z_a > \lambda$, the maximum force appears near $z_a = d_A$. This is attributed to the resonant part of the CP force, which is due to the focus effect of LHMs. In detail, as the atom is placed at $z_a = d_A$, its emitted electromagnetic field can be refocused at the same position after the field goes through the LHMs and is reflected by mirror.

We note that when the separation between the atom and surface is larger than 0.1λ, the dispersive part of the force can be ignored in comparison with the resonant part. For example, in the case of Fig. 4(a), at $z_a = \lambda$, $F_1^r(z_a)$ is about 10^5 times larger than $F_1^{or}(z_a)$ (not explicitly shown). To get a feeling of the force scale, we consider the typical atom parameters, i.e., $|d_{10}|^2 = 10^{-59}\mathrm{C}^2\,\mathrm{m}^2$, $\omega_{10} = 5.36 \times 10^{14}$, and $B \approx 3.0 \times 10^{-25}\mathrm{N}$. When we take the atomic mass to be about $10^{-27}\mathrm{kg}$, the Casimir-Polder force near the focus region can produce acceleration of the order of 10 g.

Next we consider the structure shown in Fig. 1(b), i.e., the LHM cavity. The indices of the LHM and metal are still as given in Eqs. (15) and (16). The cavity structure helps the force produce an interesting effect: The two focus points next to each other can now be used to push and trap the atom in the middle, as shown in Fig. 5. Two cases are studied here: when $d_A = 2\lambda$ with $d_0 = 6\lambda$ and when $d_A = \lambda$ with $d_0 = 3\lambda$.

In the LHM cavity, the time-independent force amplitude $F_1(z_a)$ and the decay rate $\Gamma(z_a)$ with $d_A = 2\lambda$ and $d_0 = 6\lambda$ are plotted in Fig. 5. Clearly $F_1(z_a)$ is asymmetric and $\Gamma(z_a)$ is symmetric around $z_a = 3\lambda$. The two focal points at $z_a \approx 2\lambda$ and $z_a \approx 4\lambda$ stand out, creating the possibility for the force amplitude to play a significant role. The function of the cavity structure investigated here is to provide a potential well that pushes the atom into the middle area. To illustrate this further we note that, when considering the parallel dipole case, the force in the region $z_a \in [1.8\lambda, 2.2\lambda]$ pushes the atom to the right-hand side, while the force in the region $z_a \in [3.8\lambda, 4.2\lambda]$ pushes the atom to the left-hand side. For a normal dipole, the forces in the regions $z_a \in [2\lambda, 2.5\lambda]$ and $z_a \in [3.5\lambda, 4\lambda]$ play a significant role since they push the atom into the center. This is a convenient application when it comes to trapping the excited atom in the middle of the cavity structure due to the resonant Casimir-Polder force. More importantly, the spontaneous decay of the atom in these four regions is inhibited compared to the free space case, as shown in Fig. 5(b). This means that these significant resonant Casimir-Polder forces should exist for longer times. On comparing Fig. 5 with Fig. 4, the profile of the force near the focus points in the cavity is similar to that of a single mirror. If we further shorten the length of the cavity, the maximum force should be enhanced due to the resonance of cavity. The case of the cavity with $d_A = \lambda$ and $d_0 = 3\lambda$ is plotted in Fig. 6.

The distance between the two focus points is one wavelength. It is clear that, for the parallel dipole, the maximum

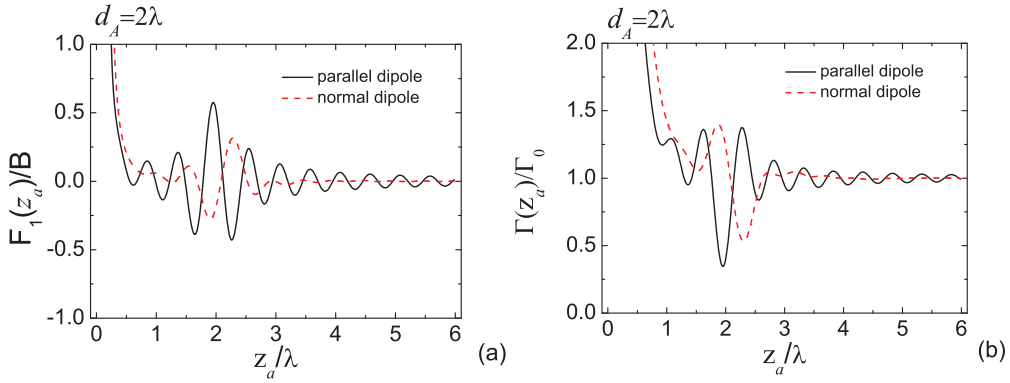

FIG. 4. (Color online) (a) Time-independent force amplitude $F_1(z_a)$ and (b) decay rate $\Gamma(z_a)$ as functions of position. The excited atom is situated near the single LHM-metal structure with $d_A = 2\lambda$ with indices given by Eqs. (15) and (16).

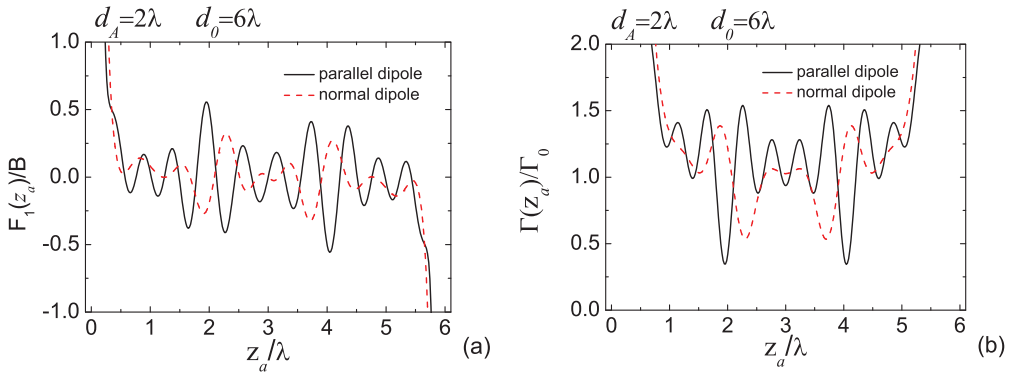

FIG. 5. (Color online) (a) Time-independent force amplitude $F_1(z_a)$ and (b) decay rate $\Gamma(z_a)$ as functions of position. The excited atom is situated in the LHM cavity with $d_A = 2\lambda$, $d_0 = 6\lambda$, and indices given by Eqs. (15) and (16).

force amplitudes are located at $z_a = 0.9\lambda$ and $z_a = 2.1\lambda$, while this happens at $z_a = 1.3\lambda$ and $z_a = 1.7\lambda$ for the normal dipole. These forces push the atom to the center of the cavity. The results are more interesting for the normal dipole, i.e., there exists a perfect potential well in the middle of the cavity in which the force is zero and its slope is negative at the center of cavity. This simply means that the bottom of the well is just at this position [red dotted line in Fig. 6(a)]. Similarly, the decay rates in the regions of significant force are inhibited [see Fig. 6(b)]. Qualitatively, the minimum decay rate of the normal dipole is larger than that of the parallel dipole, so the duration of the potential well for the excited normal dipole is shorter than that of the excited parallel dipole.

B. Left-handed materials mounted on ZIMs

Although the structure of LHMs mounted on metal can enhance the resonant part of the Casimir force on the excited atom, the force is orientation dependent. It follows that, near the focus, the force and the decay rate have opposite characteristics for parallel and normal dipoles. For example, at a certain position when the force is repulsive (positive) for the parallel dipole, it is absorptive (negative) for the normal dipole. When the decay rate is inhibited (smaller than Γ_0) for the parallel dipole, it is enhanced (larger than Γ_0) for the normal dipole and vice versa. It seems that there is a π phase difference between the force acting on the parallel dipole and the normal dipole. These characteristics should weaken the force acting on an arbitrarily orientated atom. To deal with this dilemma and clarify the odds, we now replace the metal by zero-index materials, whose indices satisfy

$$\varepsilon_M = \mu_M = 1 - \frac{(0.9997\omega_{10})^2}{\omega^2}; \tag{17}$$

the indices near the atomic transition frequency tends to zero simultaneously, i.e., $\varepsilon_M(\omega_{10}) = \mu_M(\omega_{10}) \approx 0.0001$.

The main difference between the metal and zero-index material concentrates on the reflective coefficient of TM polarization. The reflective coefficient of TM polarization is 1 on metal, but is -1 on zero-index materials. To prove this point, we consider the case of an incidence beam from the vacuum into zero-index materials. The indices are $\varepsilon_0 = \mu_0 = 1$ for the vacuum and $\varepsilon_M = \mu_M = 0$ for ZIMs. According to the Fresnel formula, the reflective coefficients of the plane wave are [38]

$$\begin{aligned} r^{TE} &= \frac{\mu_M K_Z - \mu_0 K_{MZ}}{\mu_M K_Z + \mu_0 K_{MZ}}, \\ r^{TM} &= \frac{\varepsilon_M K_Z - \varepsilon_0 K_{MZ}}{\varepsilon_M K_Z + \varepsilon_0 K_{MZ}}, \end{aligned} \tag{18}$$

where K_Z and K_{MZ} are the z components of the wave vector in the vacuum and ZIMs, respectively. They are related to each other through the parallel component of the wave vector q, i.e., $\omega^2/c^2 - K_z^2 = q^2 = \varepsilon_M\mu_M\omega^2/c^2 - K_{Mz}^2$. For ideal

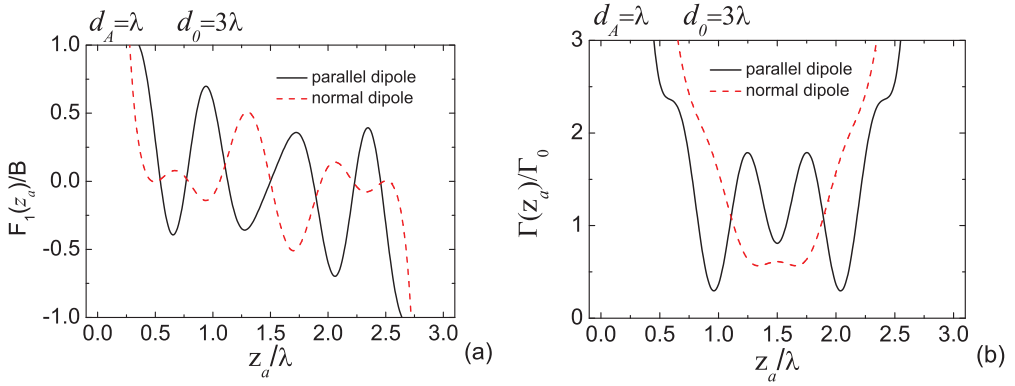

FIG. 6. (Color online) (a) Time-independent force amplitude $\mathbf{F}_1(z_a)$ and (b) decay rate $\Gamma(z_a)$ as functions of position. The excited atom is situated in the LHM cavity with $d_A = \lambda$, $d_0 = 3\lambda$, and indices given by Eqs. (15) and (16).

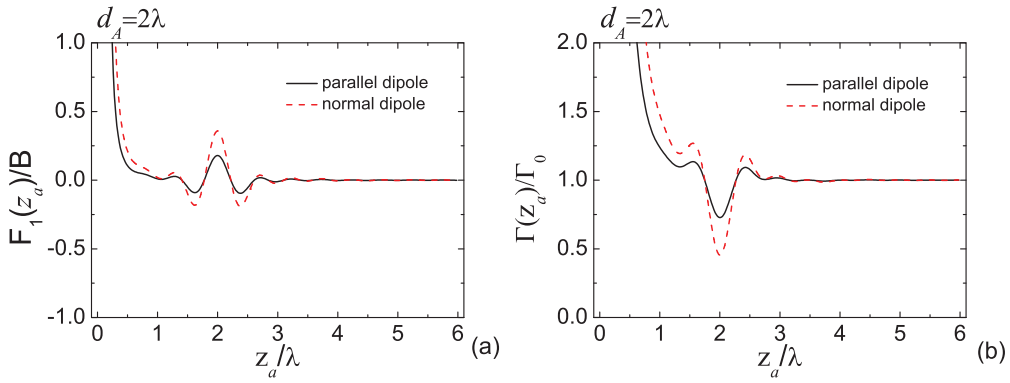

FIG. 7. (Color online) (a) Time-independent force amplitude $F_1(z_a)$ and (b) decay rate $\Gamma(z_a)$ as functions of position. The excited atom is situated near the single LHM-ZIM structure with $d_A = 2\lambda$ and indices given by Eqs. (15) and (17).

ZIMs, $\varepsilon_M = \mu_M = 0$ and K_{MZ} is purely imaginary. Therefore,

$$r^{TE} = \frac{-\mu_0 K_{MZ}}{\mu_0 K_{MZ}} = -1$$

and

$$r^{TM} = \frac{-\varepsilon_0 K_{MZ}}{\varepsilon_0 K_{MZ}} = -1$$

if $q \neq 0$, i.e., for oblique incidence. However, it can be shown that the reflection coefficients become zero for normal incidence. For ZIMs, whose indices just tend to zero, the reflection coefficient tends to -1 except for normal incidence.

These differences can significantly change the behavior of the force and the decay rate near the focus points for the parallel and normal dipoles. Here we first consider the case of Fig. 4 with the metal replaced by ZIMs with characteristics given by Eq. (17). The force amplitude and the decay rate of the atom as functions of position are shown in Fig. 7.

On comparing Fig. 7 with Fig. 4 we find that the force and the decay rate change in phase with position for both parallel and normal dipoles. The amplitude for the normal dipole is stronger than that of the parallel dipole. In particular, near the focus $z_a = d_A = 2\lambda$, the force amplitude is the strongest, while the decay rate is at the deepest inhibited point.

Next we look into the same calculation that produces Fig. 6 except the metal is replaced by ZIMs. The corresponding force and the decay rate as functions of position for different dipole orientations are shown in Fig. 8.

It is clearly shown that the force changes in phase and is positive when $z_a < 1.2\lambda$, while it is negative when $z_a > 1.8\lambda$. Therefore, the force can push the atom into the middle area in a subtle way. Such an effect is much better than that of Fig. 6, where the force changes sign frequently with position.

Next we see what happens when the cavity length is $d_0 = 6\lambda$ and the cavity mirror is made of LHMs mounted on ZIMs. The corresponding force and the decay rate are shown in Fig. 9. Clearly, the force for both parallel and normal dipoles change in phase with position. Near the two focus points at $z_a = 2\lambda$ and $z_a = 4\lambda$, the force has the strongest value and pushes the atom into the middle area, while the decay is deeply inhibited.

C. Time evolution of force

As mentioned before, the force acting on the excited atom evolves due to the spontaneous decay [see Eq. (2)]. Here we give the results of calculations showing the force evolution. We consider the case of Fig. 6 as an example, in which the atom is placed in a LHM cavity surrounded by metal with $d_A = \lambda$ and $d_0 = 3\lambda$.

From the result of Fig. 6, the time-independent force amplitude $F_1(z_a)$ and the decay rate $\Gamma(z_a)$ are sensitive to the dipole orientation. Therefore, the evolution of the force

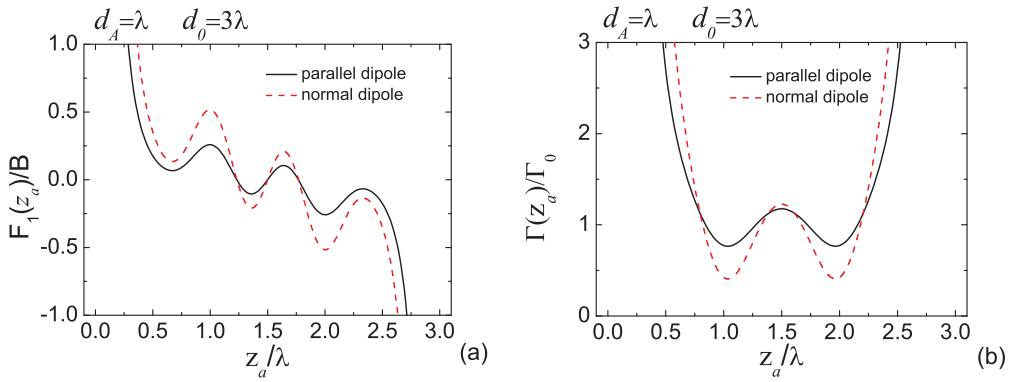

FIG. 8. (Color online) (a) Time-independent force amplitude $\mathbf{F}_1(z_a)$ and (b) decay rate $\Gamma(z_a)$ as functions of position. The excited atom is situated in the LHM-ZIM cavity with $d_A = \lambda$, $d_0 = 3\lambda$, and indices given by Eqs. (15) and (17).

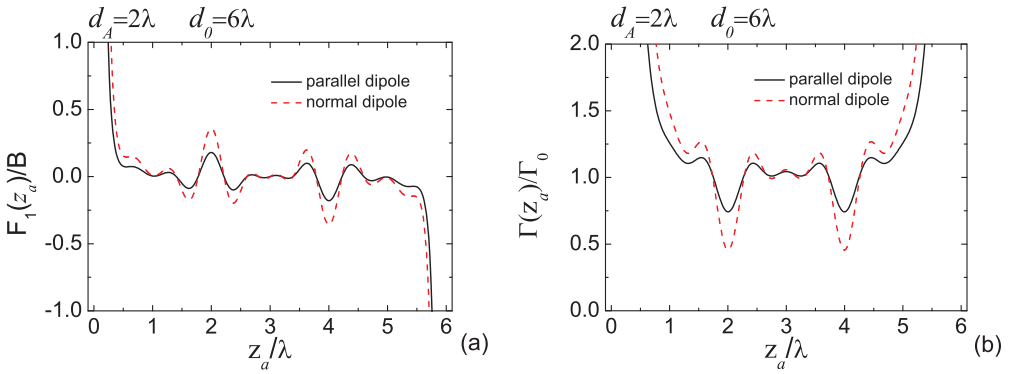

FIG. 9. (Color online) (a) Time-independent force amplitude $\mathbf{F}_1(z_a)$ and (b) decay rate $\Gamma(z_a)$ as functions of position. The excited atom is situated in the LHM-ZIM cavity with $d_A = 2\lambda$, $d_0 = 6\lambda$, and indices given by Eqs. (15) and (17).

acting on the parallel dipole has a different signature from that of the normal dipole. Details are shown in Fig. 10.

At the initial time $t = 0$, the profiles of the force (red solid curves) are just the time-independent force amplitude $F_1(z_a)$, which are the same as the curves in Fig. 6(a). With time evolution, the force near the surfaces changes sign (from positive to negative near the left surface and from negative to positive near the right surface) quickly. The reason is that the force near the surface is dominated by the dispersive part and changes sign after the atom decays to the ground state. Due to the high decay rate near the surface, at time $t = \Gamma_0/4$, the atom near the surface has already decayed to the ground state and the force takes the value of Eq. (6). However, in the middle area of the cavity, the force is dominated by the resonant part of the force and the atom decays exponentially at a different rate. As mentioned above, near the focus points, the decay rate has its minimum value when it is at the positions with the maximum force amplitude $F_1(z_a)$. However, such positions are different between the parallel dipole and the normal dipole. For the parallel dipole, at $t = 2/\Gamma_0$ [solid dark curve in Fig. 10(a)], only the force near the two focus points ($z_a = \lambda$ and $z_a = 2\lambda$) survives and pushes the atom into the middle area of the cavity. For the normal dipole, the evolution has a similar character. The forces survive near $z_a \approx 1.3\lambda$ and $z_a \approx 1.7\lambda$ [solid dark curve in Fig. 10(b)] and construct a perfect restoring force center at $z_a \approx 1.5\lambda$ after $t > 2/\Gamma_0$.

The situation of the structure made of LHMs and ZIMs is similar, but different when it comes to the evolution that is insensitive to dipole orientation. By adopting appropriate parameters we can realize the significant restoring force far from the surface.

IV. CONCLUSION

We have presented results for the Casimir-Polder force acting on an excited cold two-level atom in a structure containing metamaterials. Due to the spontaneous decay, the force is time dependent. As predicted previously, the force can be divided into two parts: the dispersive force and the resonant force. The resonant force relates only to the electromagnetic mode at the atomic transition frequency and can be significantly controlled by a well-designed surrounding. We find that, for the atom near the structure made of LHMs mounted on highly reflective materials, the force acting on the atom can be enhanced significantly even when the atom is several wavelengths away from the surface. Although the resonant CP force decays exponentially, fortunately, at the position experiencing significant force, the decay is inhibited. Therefore, the atom can be controlled by the CP force for much longer times.

Two kinds of highly reflective materials, i.e., metal and ZIMs, were analyzed in detail. For the structure of LHMs

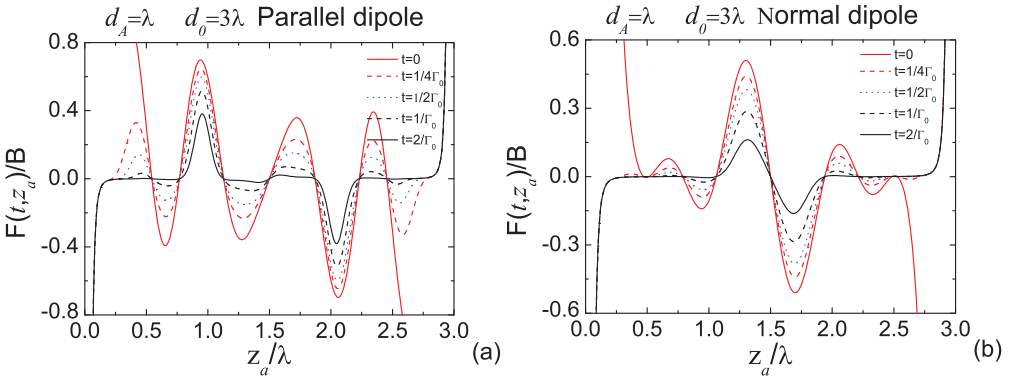

FIG. 10. (Color online) Evolution of the Casimir-Polder force for an initial excited atom in a cavity made of LHMs mounted on metal with $d_A = \lambda$ and $d_0 = 3\lambda$: atom with (a) a parallel dipole and (b) a normal dipole.

mounted on metal, near the focus point, the force acting on the atom shows opposite character for the parallel and normal dipoles. When it comes to practical situations, this weakens the mechanical effect since the atom has arbitrary orientation. To overcome this problem, we introduce another structure where the LHM is mounted on the ZIM. Due to the special reflective phenomena of ZIM, the force in this case is completely insensitive to the orientation of the atomic dipole. Near the focus points, the force on the parallel dipole has the same direction as that of the normal dipole and they reach the maximum at the same position with a lower decay rate. Furthermore, the force profile with position is smoother and does not change sign frequently. Thus, the Casimir force on an initially excited atom near the LHM mounted on the ZIM is superior to that of the LHM mounted on the metal.

With the time evolution, the significant restoring force would appear once the atom is situated in the LHM cavity. Our result has potential application in an atomic guidance system. If the atom is injected into the guide with the direction parallel to the surface, the atom can survive the absorption during its lifetime. For the Rydberg atom or some molecules with lower transition frequency, the lifetime should be much longer than the time needed to transit the guide.

In this paper we did not consider the influence of temperature on the Casimir-Polder force. Typically, thermal fluctuation should be taken into account when the distance between the atom and object is larger than one thermal wavelength [12,14,39]. In our model, the interesting distance is several wavelengths of transition frequency, therefore the influence of temperature would be considered in a realist experiment. Here we can predict several effects of temperature qualitatively, i.e., for the calculation of the dispersive part of the force, the integration over frequency in Eq. (5) would be replaced by the Matsubara summation [40]; for the resonant part of force, Eq. (6) should be multiplied by the mean thermal photon number [12]; the decay of the resonant part of the force would be accelerated due to the stimulated radiation; furthermore, the temperature would provide a statistically nonzero population of atoms, which would prolong the orientation-independent Casimir-Polder force discussed in our paper. However, a detailed analysis of quantity is beyond the scope of the present paper.

ACKNOWLEDGMENTS

This work was supported by the National Science Foundation of China (Grants No. 11274242 and No. 2012CB921603), the Joint Fund of the National Natural Science Foundation of China and the China Academy of Engineering Physics (Grant No. U1330203), NKBRSFC (Grants No. 2011CB922203 and No. 2013CB632701), the Fundamental Research Funds for the Central Universities, and a grant from KACST. The research of M.S.Z. was supported by NPRP Grant No. 4-346-1-061 from the Qatar National Research Fund.

[1] H. B. G. Casimir and D. Polder, Phys. Rev. **73**, 360 (1948).
[2] J. D. Perreault and A. D. Cronin, Phys. Rev. Lett. **95**, 133201 (2005).
[3] H. Oberst, M. Morinaga, F. Shimizu, and K. Shimizu, Appl. Phys. B **76**, 801 (2003); M. Al-Amri and M. Babiker, Phys. Rev. A **69**, 065801 (2004); Eur. Phys. J. D **48**, 417 (2008).
[4] F. Le Kien, V. I. Balykin, and K. Hakuta, Phys. Rev. A **70**, 063403 (2004).
[5] E. Buks and M. L. Roukes, Phys. Rev. B **63**, 033402 (2001).
[6] Y.-J. Lin, I. Teper, C. Chin, and V. Vuletic, Phys. Rev. Lett. **92**, 050404 (2004).
[7] V. Yannopapas and N. V. Vitanov, Phys. Rev. A **81**, 042506 (2010).
[8] G. S. Agarwal, Phys. Rev. Lett. **32**, 703 (1974).
[9] J. M. Wylie and J. E. Sipe, Phys. Rev. A **32**, 2030 (1985).
[10] D. P. Fussell, R. C. McPhedran, and C. Martijn de Sterke, Phys. Rev. A **71**, 013815 (2005).
[11] A. Sambale, S. Y. Buhmann, H. T. Dung, and D.-G. Welsch, Phy. Rev. A **80**, 051801(R) (2009).
[12] S. A. Ellingsen, S. Y. Buhmann, and S. Scheel, Phys. Rev. A **84**, 060501 (2011).
[13] S. Y. Buhmann and D.-G. Welsch, Prog. Quantum Electron. **31**, 51 (2007).
[14] S. A. Ellingsen, S. Y. Buhmann, and S. Scheel, Phys. Rev. A **79**, 052903 (2009).
[15] H. Failache, S. Saltiel, M. Fichet, D. Bloch, and M. Ducloy, Phys. Rev. Lett. **83**, 5467 (1999); Eur. Phys. J. D **23**, 237 (2003).
[16] V. G. Veselago, Sov. Phys. Usp. **10**, 509 (1968).
[17] J. B. Pendry, Phys. Rev. Lett. **85**, 3966 (2000).
[18] J. Kästel and M. Fleischhauer, Phys. Rev. A **71**, 011804 (2005).
[19] A. Alù, M. G. Silveirinha, A. Salandrino, and N. Engheta, Phys. Rev. B **75**, 155410 (2007).
[20] R. Liu, Q. Cheng, T. Hand, J. J. Mock, T. J. Cui, S. A. Cummer, and D. R. Smith, Phys. Rev. Lett. **100**, 023903 (2008).
[21] S. Enoch, G. Tayeb, P. Sabouroux, N. Guérin, and P. Vincent, Phys. Rev. Lett. **89**, 213902 (2002).
[22] V. C. Nguyen, L. Chen, and K. Halterman, Phys. Rev. Lett. **105**, 233908 (2010).
[23] X. Huang, Y. Lai, Z. H. Hang, H. Zheng, and C. T. Chan, Nat. Mater. **10**, 582 (2011).
[24] L.-G. Wang, Z.-G. Wang, J.-X. Zhang, and S.-Y. Zhu, Opt. Lett. **34**, 1510 (2009).
[25] V. Yannopapas and A. Vanakaras, Phys. Rev. B **84**, 045128 (2011).
[26] E. J. R. Vesseur, T. Coenen, H. Caglayan, N. Engheta, and A. Polman, Phys. Rev. Lett. **110**, 013902 (2013).
[27] A. Sambale, D.-G. Welsch, H. T. Dung, and S. Y. Buhmann, Phys. Rev. A **78**, 053828 (2008).
[28] Y.-P. Yang, J.-P. Xu, H. Chen, and S.-Y. Zhu, Phys. Rev. Lett. **100**, 043601 (2008).
[29] V. Yannopapas, E. Paspalakis, and N. V. Vitanov, Phys. Rev. Lett. **103**, 063602 (2009).
[30] S. Evangelou, V. Yannopapas, and E. Paspalakis, Phys. Rev. A **83**, 055805 (2011).
[31] Y.-P. Yang, R. Zeng, J.-P. Xu, and S.-T. Liu, Phys. Rev. A **77**, 015803 (2008); Y.-P. Yang, R. Zeng, H. Chen, S.-Y. Zhu, and

M. S. Zubairy, *ibid.* **81**, 022114 (2010); R. Zeng and Y.-P. Yang, *ibid.* **83**, 012517 (2011).

[32] J.-P. Xu, Y.-P. Yang, and S.-Y. Zhu, J. Mod. Opt. **57**, 1473 (2010).

[33] Y.-P. Yang, J.-P. Xu, H. Chen, and S.-Y. Zhu, Phys. Rev. A **82**, 030304(R) (2010).

[34] J.-P. Xu, M. Al-Amri, Y.-P. Yang, S.-Y. Zhu, and M. S. Zubairy, Phys. Rev. A **84**, 032334 (2011).

[35] H. T. Dung, S. Y. Buhmann, L. Knöll, D. G. Welsch, S. Scheel, and J. Kästel, Phys. Rev. A **68**, 043816 (2003).

[36] T. Koschny, P. Markos, D. R. Smith, and C. M. Soukoulis, Phys. Rev. E **68**, 065602(R) (2003).

[37] T. Koschny, P. Markos, E. N. Economou, D. R. Smith, D. C. Vier, and C. M. Soukoulis, Phys. Rev. B **71**, 245105 (2005).

[38] M. Born and E. Wolf, *Principles of Optics* (Cambridge University Press, Cambridge, 1999).

[39] C. Henkel, K. Joulain, J.-P. Muler, and J.-J. Greffet, J. Opt. A **4**, S109 (2002).

[40] M. Bordag, U. Mohideen, and V. M. Mostepanenkoc, Phys. Rep. **353**, 1 (2001).